

Velocities of surface acoustic waves in proton exchanged lithium niobate with different $H_xLi_{1-x}NbO_3$ phases

D. Čiplys¹, R. Rimeika¹, Yu. V. Korkishko², V. A. Fedorov²

¹ Vilnius University, Laboratory of Physical Acoustics, Physics Faculty, Saulėtekio 9, 2054 Vilnius, Lithuania

² Moscow Institute of Electronic Technology, Engineering University, Department of Chemistry, 103498 Moscow, Zelenograd, Russia

Introduction

Proton exchange in lithium niobate has become an attractive method for the fabrication of optical and acoustic waveguides to be used in integrated optics and acoustooptics. The term “exchange” means that a great amount (up to 70 %) of Li^+ ions in the initial lattice of the crystal are replaced by H^+ ions. The exchange is usually performed by immersing the $LiNbO_3$ substrate into a hot acid melt for a certain time. The acid serves as the source of protons and accepts lithium. As a result, $H_xLi_{1-x}NbO_3$ layer of thickness of several microns is formed at the surface of the initial substrate. This layer possess physical properties different from those of the substrate enabling the optical and acoustic waveguiding. The exchange is frequently followed by annealing, mostly in air as an ambient atmosphere. Depending on the acidity of the proton source, as well on the temperature and duration of the exchange and annealing, the properties of formed waveguide layers vary in a large scale. Thus, it seems important to look for new methods enabling to monitor the characteristics of fabricated $H_xLi_{1-x}NbO_3$ layers. In the present paper, the possibilities of using surface acoustic waves for characterisation of different proton-exchanged $LiNbO_3$ samples are studied. It is known that the SAW velocity is sensitive to the properties of the layer at the crystal surface, and, when measuring the velocity, one could expect different responses from differently fabricated PE layers.

Samples

A great variety of acids can be used as the source of protons in the exchange procedure. Very frequently benzoic acid which acidity can be reduced by adding up to 5% of lithium benzoate is used. Also the solution of $KHSO_4$ in glycerine, pyrophosphoric acid, and ammonium dihydrophosphate ($NH_4H_2PO_4$) enable to obtain PE layers with very different characteristics [1]. It is important to note that the structure of resulting $H_xLi_{1-x}NbO_3$ layers depends on their formation conditions and exhibits a rather complex behaviour. Up to seven crystallographic $H_xLi_{1-x}NbO_3$ phases have been observed. Each phase is characterised by its specific dependence of the surface refractive index enhancement Δn_s upon the normal strain component ε_{33} of the layer. The strains in the layer appear as a result of the change in lattice parameters as the ion of

one type is substituted by the ion of another type. The strains normal to the substrate surface are shown to be prevailing. The structural phase diagram of Z-cut proton-exchanged $LiNbO_3$ is shown in Fig. 1, where the enhancement of refractive index Δn_s is plotted as a function of the normal strain component ε_{33} (lines). More detailed discussion on different phases and relevant sample preparation conditions can be found elsewhere [1]. Here it is important to us to show the positions of the samples chosen for studies in the diagram (dots). One can see that they represent a wide variety of different crystallographic phases.

In order to determine the position of the sample in the

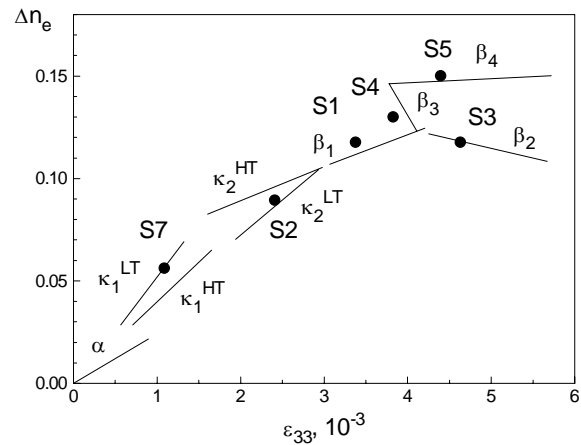


Fig. 1. Structural phase diagrams of $H_xLi_{1-x}NbO_3$ on Z-cut $LiNbO_3$ substrate. The notation of phases according to [1] is used

diagram, the refractive index profiles of the samples, as usually, were found from the measured spectra of guided optical mode effective refractive indices by the inverse WKB procedure, and the strains ε_{33} were evaluated from X-ray diffraction measurements using the rocking curves method. The refractive index profiles for each sample named S1, S2, S3, S4, S5, and S7 are shown in Fig. 2. Different phases existing in the layer can be recognised from the rocking curves, and each of them appears as a sublayer. The boundaries between the regions of different phases in the layers are shown in Fig. 2 too. One can see that a single phase layer is obtained only in the S1 sample whereas the other layers are multiphase ones.

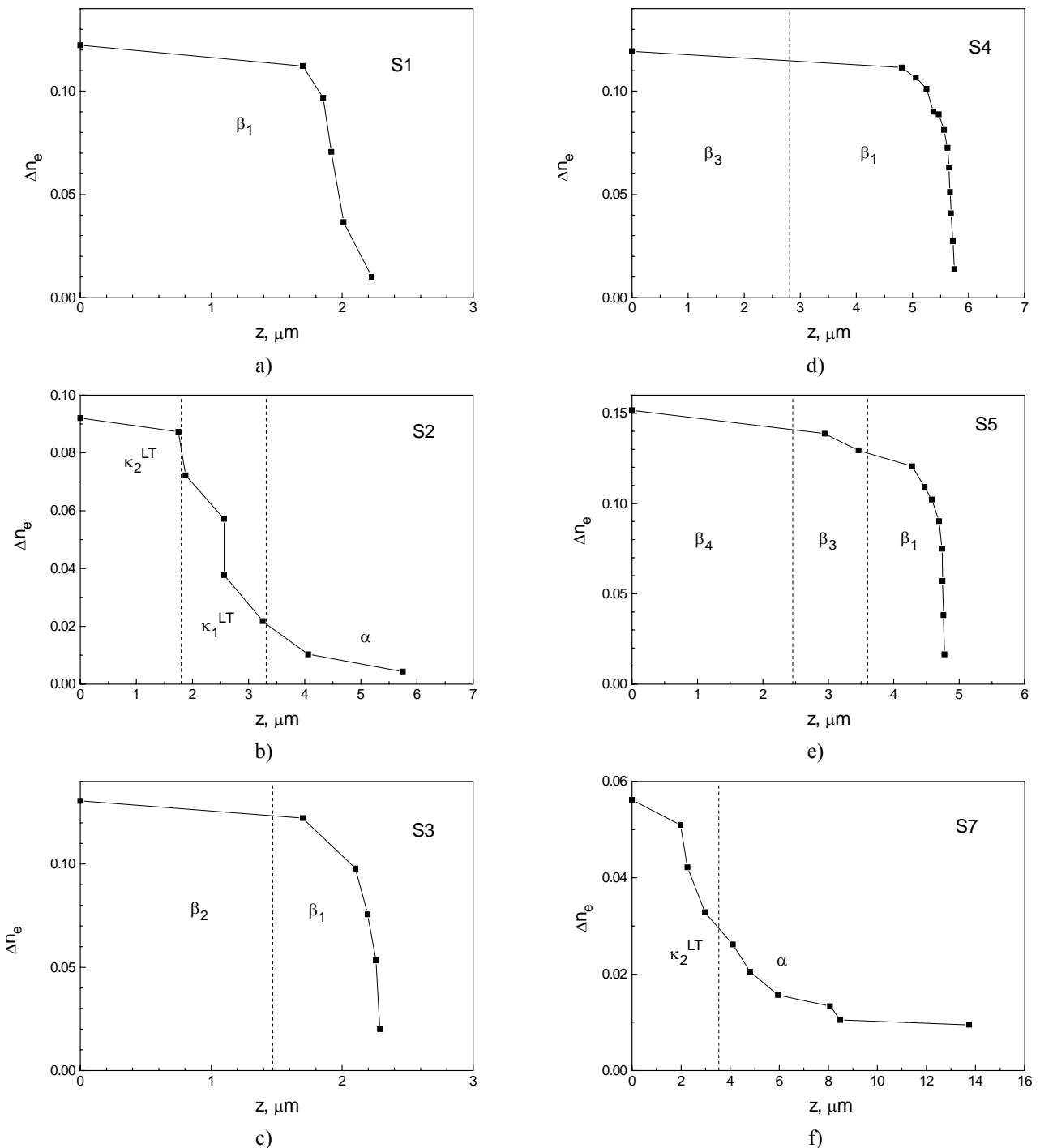


Fig. 2. Refractive index profiles of PE :LiNbO₃ samples studied . Dashed lines show the borders between different phases.

SAW velocity measurement techniques

The surface acoustic waves were excited by interdigital transducers which were deposited on areas protected from the proton exchange. The transducers with a grating period 30 μm and 60 μm were used and they could operate at their fundamental and higher harmonics, thus covering the range of frequencies from 60 to about 400 MHz. The input transducer was fed by r.f. pulses of about 1 μs duration, and the propagating of the SAW was monitored by the probe beam from He Ne laser with the wavelength 0.6328 μm . The angle 2Δ between +1 and -1

orders of the acoustooptic diffraction was measured, and the SAW velocity was determined from the relation

$$V = \frac{f\lambda}{\left(1 - \frac{\sin^2 \Theta_0}{\cos^2 \Delta}\right)^{1/2} \sin \Delta},$$

where Θ_0 was the angle of incidence of the light. The measurement of the angles was performed by the precise goniometer, and the error in the velocity value typically did not exceeded 0.1 % (approximately 4 m/s), except special cases of several points where the error grew up to 10 m/s.

Pure sample

In order to check the experimental set-up, the measurements were carried out in non-exchanged sample. Results of our measurements are compared with the literature data [2] in the Table 1.

Table 1. SAW velocity, m/s

Propagation direction	Our data	Literature data
ZX	3796	3798
ZY	3897	3903

Values taken from [2] present the results of calculations performed using the elastic, piezoelectric and dielectric constants of the LiNbO₃ crystal independently determined by other authors. Our experimentally measured values are in a good agreement with them.

Velocity in PE samples

The dependencies of SAW velocity upon frequency on the surfaces subjected to the proton exchange are presented in Figs. 3 and 4 for SAW propagation along X and Y crystallographic axes, respectively.

In accordance with the previous studies [3,4], the well expressed dispersion is observed. The velocity decreases with the frequency both for the X and Y directions. At $f \rightarrow 0$, the SAW velocity tends to its value in pure LiNbO₃. At highest frequencies, about 400 MHz, no saturation is attained since the SAW energy is still distributed between a layer and a substrate. The acoustic wavelength (and the characteristic penetration depth) at 400 MHz is of the order of 10 μm whereas the thickness of the thickest proton exchange layer is about 5 μm .

Dependencies on kd

The reason for the SAW dispersion observed is the existence of the layer at the sample surface which has acoustic properties different from those of the bulk of the sample. The term “acoustic properties” means the set of physical parameters which describe the SAW propagation

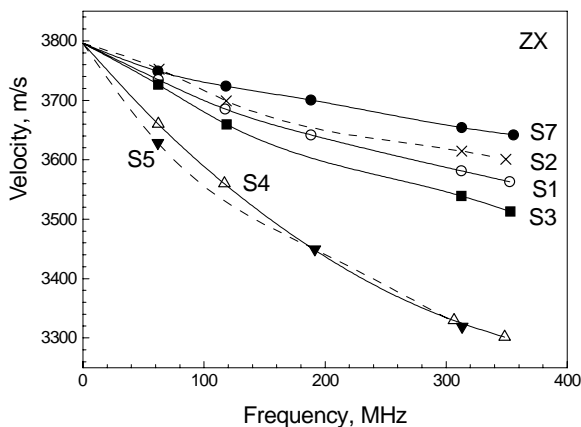


Fig. 3. SAW velocity vs frequency in PE Z-cut LiNbO₃ for X propagation direction.

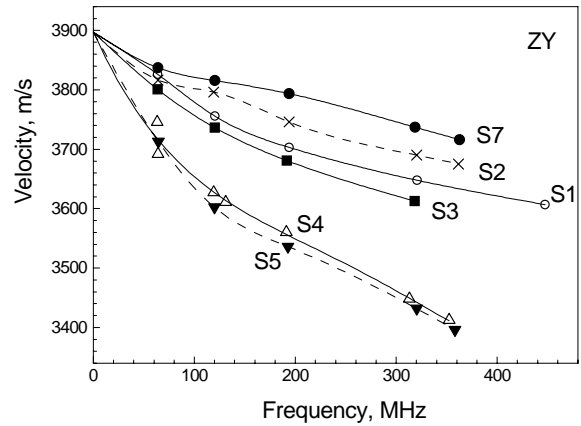


Fig. 4. SAW velocity vs frequency in PE Z-cut LiNbO₃ for Y propagation direction.

in a layered structure. Namely, these are:

- tensor of elastic constants, c_{ijkl} ;
- mass density, ρ .

In piezoelectric materials, tensor of piezoelectric constants, e_{ijk} , tensor of dielectric permittivities, ϵ_{ij} , must be included, though the influence of these terms seems to be much weaker.

It should be pointed out that we do not know *a priori* if our layers are acoustically homogenous, consist of several sub-layers, or their acoustic properties are continuously varying depth functions. Moreover, we do not know what are the real profiles of hydrogen and other atoms concentrations which are the cause of the change in acoustic properties. All we possess are the profiles of refractive indices, and let us consider our results on this basis.

In the samples S1, S3, S4, S5 the index profiles are close to step-like function, and, in contrary, they are far from this form in the samples S2, S7. Nevertheless, in order to compare the results obtained in different samples, a common parameter should be defined. Let us define the effective layer thickness as follows: it is the thickness of the step which has the height equal to the refractive index value at the very surface n_s , and the area equal to the area of real profile. It is evident that such a definition is a good approximation for the samples S1, S3, S4, S5, and it serves only as a rough approximation for S2, S7. The effective layer thicknesses thus obtained are listed below in Table 2.

Table 2. Characteristic parameters of the samples

Sample	S1	S2	S3	S4	S5	S7
Effective layer thickness $d, \mu\text{m}$	1.85	2.85	2.14	5.43	4.29	2.89
Change in surface refractive index, n_s	0.12	0.093	0.12	0.12	0.15	0.056

Using the layer thicknesses thus obtained we were able to normalise the experimental results shown in Fig. 3 and 4 with respect to common parameter kd , where k is the acoustic wavenumber. The dependencies of the relative

velocity change $\Delta V/V$ upon kd are shown both for Y and X directions in Fig. 5 and Fig. 6, respectively.

The relative velocity change is expressed in per cent unities with respect to the velocity in pure LiNbO_3 . One can see from Fig. 5 and 6 that the dependencies $V(kd)$ for samples S1, S3, and S4 coincide both for the X and Y directions. This is an evidence that the layers of different thicknesses in S1, S2, and S4 have the same acoustic properties, hence, they are homogenous and the phases β_1 , β_2 , β_3 can not be acoustically distinguished. Thus, the layers can be characterised by the single set of acoustic parameters which under certain assumptions may be evaluated from the best fit of the measured and calculated values of the SAW velocity. A stronger dispersion is observed in the sample S5, and this can be treated as an addition of the acoustically different β_4 sublayer. We must deal here with a two-layers-on-substrate system, and, at the moment, it is not clear if it is possible to determine unambiguously the parameters of the sublayer.

Weaker dispersion is observed in the samples S2 and S7 which were post-exchange annealed. This shows that, in general, the acoustic properties (elastic constants, in

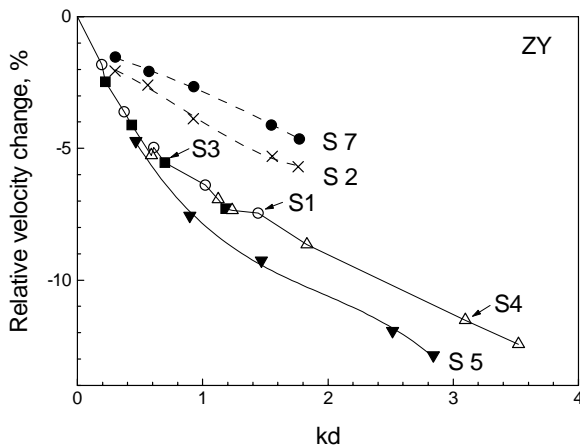


Fig. 5. Relative change in SAW velocity vs wavenumber-thickness product for various PE samples; Y propagation.

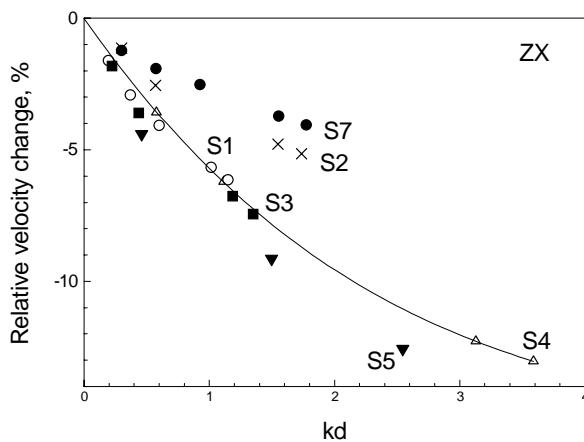


Fig. 6. Relative change in SAW velocity vs wavenumber-thickness product for various PE samples; X propagation.

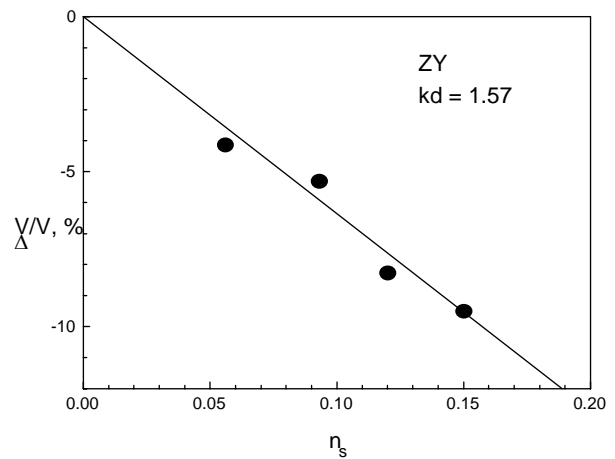


Fig. 7. Relative change in SAW velocity vs enhancement of surface refractive index at constant kd . Samples S1, S3, S4, S5.

particular) are closer to those of the pure crystal as compared with the samples S1, S2, S4, and S5. What concerns the evaluation of acoustic parameters, the possibility of their depth dependence should be taken into account what makes the situation rather complicated.

It should be noted that, for a given sample, the dependencies of relative velocity change upon kd for X and Y directions are quite similar. Such a feature for Z-cut sample is different from that for Y-cut sample [5] where a different behaviour of $V(kd)$ curves for X and Z propagation cases has been observed.

A certain correlation between the SAW velocity change and the refractive index enhancement due to the proton exchange can be noticed. It is demonstrated in Fig 7 where the dependence of relative change in the SAW velocity is plotted upon Δn_s for Y propagation direction at the fixed $kd = 1.57$ value corresponding to the condition $d = \lambda / 4$.

Conclusions

The surface acoustic velocity being sensitive to the properties of the surface layer of the crystal can serve as a tool for characterisation of proton-exchanged LiNbO_3 waveguides fabricated at different conditions. The formation of $\text{H}_x\text{Li}_{1-x}\text{NbO}_3$ layer causes the strong acoustic dispersion. No differences in the dispersion were observed in the samples with β_1 , β_2 , β_3 phases, showing that they are identical from the acoustic point of view, whereas the appearance of β_4 phase leads to stronger dispersion. The phases κ which are obtained in annealed samples are characterised by much weaker dispersion.

References

1. Yu. N Korkishko, V. A Fedorov. Structural phase diagram of $\text{H}_x\text{Li}_{1-x}\text{NbO}_3$ waveguides: the correlation between optical and structural properties// IEEE Journ. of Selected Topics in Quantum Electronics.- 1996. Vol. 2.- P. 187-196.
2. A. J. Jr. Slobodnik, E. D. Conway, R. T Delmonico. Microwave acoustics handbook// 1973.-Vol.1A. -Air Force Cambridge Research Laboratories.- USA.- P.406.

3. **V Hinkov, E. Ise.** Surface acoustic waves velocity perturbation in LiNbO_3 by proton exchange// Appl. Phys. Lett.- 1985. Vol. 18- P.31-34.
4. **J. Paðkauskas, R. Rimeika and D. Èiplys.** Velocity and attenuation of surface acoustic wave in proton-exchanged 128° - rotated Y-cut LiNbO_3 // Journ. Phys. D: Appl. Phys.- 1995.- Vol. 28.- P. 419-1423.
5. **M. E. Biebl and P. Russer.** Elastic properties of proton exchanged lithium niobate//IEEE Trans. Ultrason. Ferroel. Freq. Control.- 1992.- Vol. 39.- P. 330-334.

D. Čiplys, R. Rimeika, Yu. V. Korkishko, V. A. Fedorov

Paviršinių akustibnių bangų greičiai protonų mainų ličio niobate esant skirtingoms $\text{H}_x\text{Li}_{1-x}\text{NbO}_3$ fazėms

Reziumė

Ištirtos galimybės panaudoti paviršines akustines bangas skirtingų protonų mainų LiNbO_3 sluoksnių charakteristikoms apibūdinti. Priklausomai nuo protonų šaltinio rūgštingumo, nuo mainų ir iškaitinimo procesų trukmės bei temperatūros, suformuotų šviesolaidinių sluoksnių savybės gali būti labai įvairios. Buvo ištirti bandiniai su septyniomis $\text{H}_x\text{Li}_{1-x}\text{NbO}_3$ fazėmis. PAB greitis buvo akustiškai ir optiškai matuojamas dažnių ruože nuo 60 iki 400 MHz. Suformuotas $\text{H}_x\text{Li}_{1-x}\text{NbO}_3$ sluoksniuose sąlygoja stiprią akustinę dispersiją. Dispersija buvo vienoda bandiniuose su β_1 , β_2 , β_3 fazėmis, ir tai rodo, kad akustiniu požiūriu jos yra identiškos. Fazės β_4 susidarymas sąlygoja stipresnę dispersiją. Fazių β_4 kurios susidaro tik iškaitinus bandinius, dispersija daug silpnesne.